Journal of Power Sources 240 (2013) 14–17

Contents lists available at SciVerse ScienceDirect

Journal of Power Sources

journal homepage: www.elsevier.com/locate/jpowsour

Short communication

Evaluation and analysis of Li-air battery using ether-functionalized ionic liquid

Shougo Higashi [a,*], Yuichi Kato [a], Kensuke Takechi [a], Hirofumi Nakamoto [b], Fuminori Mizuno [b], Hidetaka Nishikoori [b], Hideki Iba [b], Takahiko Asaoka [a]

[a] Electrochemistry Div., Toyota Central R&D Laboratories, Inc., 41-1 Nagakute, Aichi 480-1192, Japan
[b] Battery Research Div., TOYOTA Motor Corporation Higashifuji Technical Center, 1200 Mishuku, Susono, Shizuoka 410-1193, Japan

HIGHLIGHTS

- Discharge capacity was improved by using DEME-TFSA compared with PP13-TFSA.
- After discharge, 4 $f\hat{E}$m diameters aggregates are formed on the surface of cathode.
- Almost 80% of the discharged products are decomposed after charge.
- Two typical peaks attributed to Li_2O_2 were detected from the discharged products.
- Discharged products were not decomposed completely by charge.

ARTICLE INFO

Article history:
Received 17 December 2012
Received in revised form
25 February 2013
Accepted 1 March 2013
Available online 28 March 2013

Keywords:
Lithium-air
Battery
Ionic liquid
Lithium
Superoxide

ABSTRACT

Li-air battery using ionic liquids, *N*,*N*-diethyl-*N*-methyl-*N*-(2-methoxyethyl) ammonium bis (trifluoromethylsulfonyl) amide (DEME-TFSA) and *N*-methyl-*N*-propylpiperidinium bis(trifluoromethanesulfonyl)amide (PP13-TFSA), as the solvents for electrolyte have been studied. A significant improvement of discharge capacity has been observed for DEME-TFSA (4315 mAh g^{-1}-electrode at current density of 0.1 mA cm^{-2}), compared with PP13-TFSA. As a discharged product, aggregates reaching 4 μm diameter in size are formed on the surface of cathode, almost 80% of the products are decomposed after charge. By using Raman spectroscopy, two typical peaks attributed to Li_2O_2 were detected from the discharged aggregates. From the cross sectional SEM images, vacancy occupation ratios of discharged and charged electrodes are estimated, and they are in good agreement with the theoretical calculations. The discharged products formed inside of the cathode are not decomposed completely by charge.

1. Introduction

The risk of running out of the conventional fossil fuel is threatening the economic growth [1]. Although many of the prominent alternative renewable energies have been proposed and devised such as, solar, wind, tidal and hydrogen energy systems, human kind has not yet achieved the system that allows us to store large amount of the generated energy effectively, wasting as the surplus electricity. In order to effectively store large amounts of the generated energy resulting from fossil fuel use, energy storage systems with high energy capacity are required. Among the renovative battery systems proposed, lithium-air battery is one of the most promising candidates for future energy storage system which can be applicable to the electric vehicles because of its large theoretical capacity [2–4]. Since the prototype system of rechargeable Li-air battery proposed [5,6], many researchers have been attracted by this electrochemical system [7]. Recently, an important fact has been revealed, that is, the super oxide anion radical ($O_2^{\bullet -}$) formed during the discharge attacks and decomposes the non-aqueous organic electrolyte such as propylene carbonate (PC) which is often used in Li-air battery [8]. The decomposition of the electrolyte causes the severe deterioration of its battery performance. Thus exploration of a stable electrolyte has been become of one of the most important challenges, and of crucial for realization Li-air secondary battery [9,10].

To meet this requirement, we have proposed a method for screening the appropriate solvents stable against $O_2^{\bullet -}$ (KO_2 screening) for the Li-air battery's electrolytes [11,12]. The method exploits the property of KO_2 which is dissociated into $K^+ + O_2^{\bullet -}$ in solvents. Using the method, PP13-TFSA (Fig. 1) is found to be the

* Corresponding author.
E-mail address: shigashi@mosk.tytlabs.co.jp (S. Higashi).

0378-7753/$ – see front matter © 2013 Elsevier B.V. All rights reserved.
http://dx.doi.org/10.1016/j.jpowsour.2013.03.008

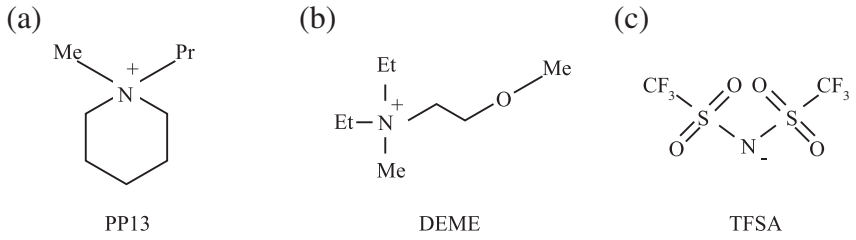

Fig. 1. Schematic illustrations of the molecular structures of cations and anions of room temperature ionic liquids. (a) *N*-methyl-*N*-propylpiperidinium (PP13), (b) *N*,*N*-diethyl-*N*-methyl-*N*-(2-methoxyethyl)ammonium(DEME), (c)bis(trifluoromethanesulfonyl)amide(TFSA).

most stable and suitable as the electrolyte of the Li-air battery. Our group has shown that the large voltage gap of discharge and charge, often observed for carbonate based electrolyte due to the decomposition of electrolyte, is suppressed by using PP13-TFSA, and successfully confirmed the formation of Li_2O_2 as a discharged product [8,12]. However, battery performance of Li-air battery with PP13-TFSA was limited most likely because of its relatively high viscosity, results in the low oxygen diffusion in the solvent. In this report, we show the battery performance of Li-air battery using ionic liquid, DEME-TFSA (Fig. 1), which has a lower viscosity than the PP13-TFSA [13], and results of Raman spectroscopy of discharged products, and of SEM observations of the cathode at various battery conditions.

2. Experimental

A roll pressed sheet type electrode with a thickness of 80 μm consists of 80 wt% Ketjen-black (ECP-600JD) and 20 wt% of PTFE punched out ϕ18 mm in size is used as the cathode and for anode same size of 400 μm thick Li foil was used. For the battery cell evaluation, Li-air battery cells filled with O_2 gas (0.1 MPa) were used. As the electrolytes, DEME-TFSA and PP13-TFSA containing 0.32 mol kg^{-1} Li-TFSA [14] were used. All charge–discharge measurements were carried out at 60 °C. After the charge–discharge measurements, cathodes are dipped into the dimethylsulfoxide (DMSO) and chloroform for 30 min, respectively. This procedure is repeated 3 times so that the electrolytes and Li-salt are removed. These processes are performed in the Ar gas filled glove box. After drying the sample in vacuum, SEM observations (NB5000, HITACHI-HITEC) and Raman spectroscopy (NRS-3300, JASCO) analyses were carried out under the Ar gas atmosphere.

3. Results and discussion

Fig. 2 show the discharge–charge curves of the Li-air batteries using PP13-TFSA and DEME-TFSA, taken at the current density of 0.1 and 0.05 mA cm^{-2} for discharge and charge, respectively. As described above, large over-potential can be observed for the case of conventional organicliquid electrolytes such as PC-based solvents during the charge, due to the decomposition of electrolyte [15]. On the other hand, by using the ionic liquids, PP13-TFSA and DEME-TFSA, the large over potential during the charge is successfully suppressed for both cases, suggesting the suppression of decomposition of electrolyte. As for the discharge capacity, the significant difference between PP13-TFSA and DEME-TFSA are observed as seen in Fig. 2. The discharge capacity of Li-air battery with DEME-TFSA reaches more than 4500 mAh g^{-1}-electrode twice as high as the PP13-TFSA case. The reason of the high discharge capacity can be understood by its high O_2 diffusion coefficient and low viscosity for the DEME-TFSA [13].

In Fig. 3, the discharge rate capabilities of PP13-TFSA and DEME-TFSA are shown. Even at the current density of 0.2 mA cm^{-2}, capacity retains more than 2500 mAh g^{-1}-electrode in the case of DEME-TFSA whereas PP13-TFSA shows 1500 mAh g^{-1}-electrode. For both cases, discharge capacity is limited at the current densities more than 0.5 mA cm^{-2}.

Next, we show the results of investigations for the transition of morphology of discharged products on the surfaces of cathode by using SEM (Fig. 4). For the discharged sample, scale-like aggregates reaching 4 μm diameter in size are observed as shown in Fig. 4(a), randomly formed on the surface of cathode and about 80% of the aggregates are disappeared by charge (Fig. 4(b)). In the discharge–

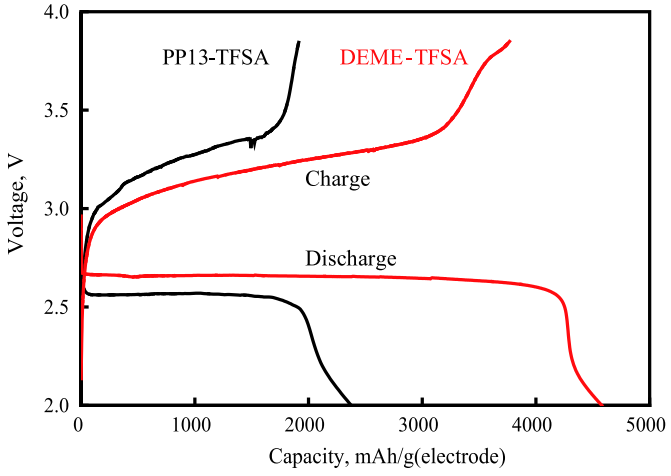

Fig. 2. Discharge–charge profiles of the Li-air battery with PP13-TFSA and DEME-TFSA taken by current density of 0.1 mA cm^{-2} at 60 °C for both charge and discharge.

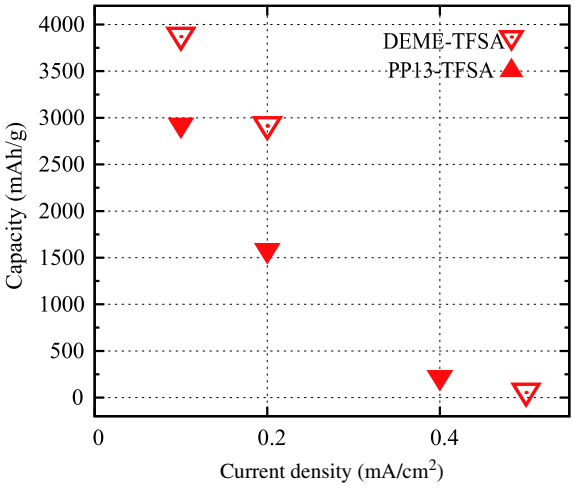

Fig. 3. Discharge rate capabilities of Li-air battery with PP13-TFSA and DEME-TFSA at 60 °C.

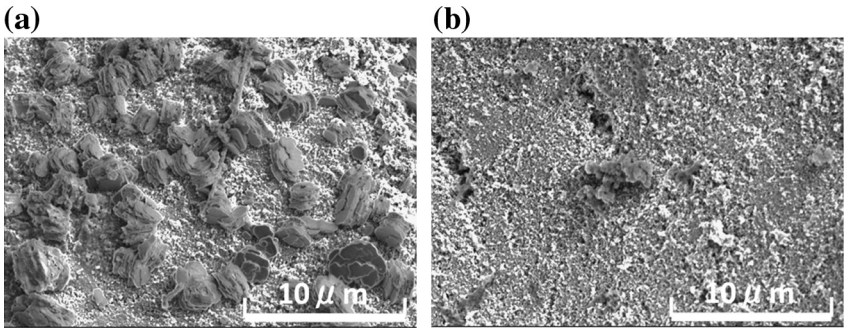

Fig. 4. SEM images of positive electrode. (a)1st discharge (b) 1st charge.

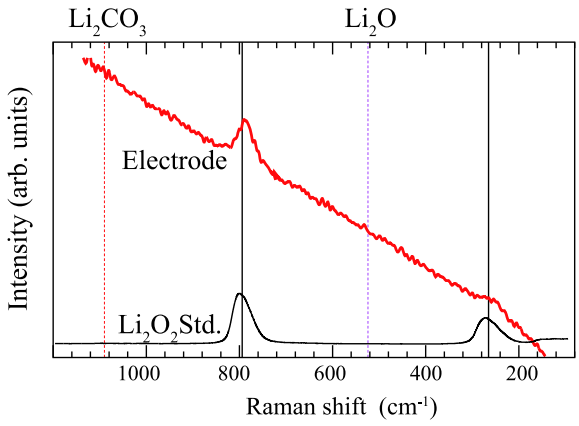

Fig. 5. Raman spectrum of standard Li_2O_2 powder and discharged electrode.

charge profile (Fig. 2), about 80% of discharge capacity was reversible, and thus these results are consistent.

Raman spectroscopy analysis is carried out to identify the chemical composition of discharge products taken. For identification standard, Raman spectrum of Li_2O_2 (90%, Aldrich) is also obtained. As seen in Fig. 5, Li_2O_2 have characteristic peaks at 785 and 287 cm^{-1}, and we also detect those two peaks from discharged electrode. The peaks of Li_2O (524 cm^{-1}), Li_2CO_3 (1091 cm^{-1}), LiOH (3662 cm^{-1}) are not observed in this study, suggesting that the major part of discharged products is Li_2O_2.

In the case of Li-air battery, discharged product (Li_2O_2) is expected to be formed inside of the cathode, namely vacant space of porous carbon, thus the observations of the change of occupancy ratio of the vacant space give important informations. Therefore, we took the cross sectional SEM images of cathodes at various battery conditions as shown in Fig. 6. The images are taken at the 30 μm deep from the surface of cathode. For a quantitative analysis, obtained images are binarized as shown in the second row of Fig. 6. White and black represent the unoccupied and occupied spaces, respectively. For comparison, SEM images of before-discharge (pristine) cathode is also shown. From the binarized images, we estimate roughly the occupation ratio of vacant space for discharged and charged samples, summarized in Table 1.

In this study, the vacancy occupation ratios are calculated simply as follows,

$$\text{Occupation ratio} = \frac{V_p - V_{\text{exp}}}{V_p} \times 100(\%), \tag{1}$$

where V_p is the white (vacant) area of pristine (before discharge) electrode, and V_{exp} is the white area for the electrode of after discharge or charge. Since we know the porosity of carbon black, weight of the electrode and discharge–charge capacity (4312 and 2728 mAh g^{-1}-electrode for discharged and charged samples, respectively), we can calculate the ideal occupation ratio from the experimental discharge–charge profile by assuming that the discharged products are all consist of Li_2O_2.

After the 1st discharge, the occupation ratio of about 50% close to theoretical value is obtained. In spite of its very large discharge capacity, the result indicates that the electrode has more space for the formation of Li_2O_2. Although the reason for the existence of unoccupied site is not clear at this time, it is presumably because of

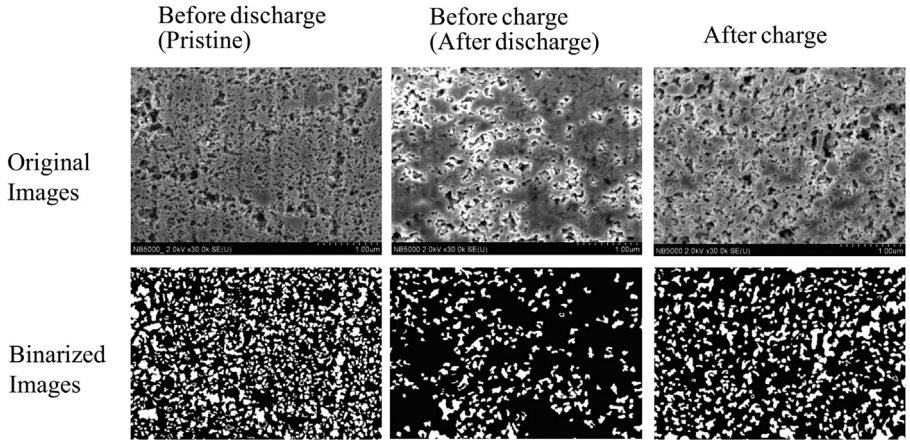

Fig. 6. Cross sectional SEM images of positive electrode taken at before discharge, before charge and after charge with binarized SEM images.

Table 1
Summary of occupation ratios of electrodes, after discharge and charge.

	After discharge	After charge
Occupation of vacancy	51%	19%
Calculated occupation From discharge/charge capacity	54%	13%

the formation of dense Li_2O_2 covering the cathode surface. The formed Li_2O_2 blocks the oxygen diffusion into inside of the cathode and limits the discharge capacity. To develop appropriately designed cathode macro-structure for improvements of the Li-air battery performances, we need to understand the mechanism of the growth process of insulating Li_2O_2. After charge, the occupation ratio becomes 19%. This is qualitatively consistent with the fact that there is an irreversible capacity as seen in discharge–charge profile. In order to suppress the irreversible capacity, an identification of chemical composition of remained discharge products after charge is required.

4. Conclusions

Lithium air battery with DEME-TFSA based electrolyte has been studied. We have found that the adaptation of DEME-TFSA based electrolyte results in the large discharge capacity, reaches more than 4500 mAh g^{-1}-electrode and discharge rate capability is also improved compared with PP13-TFSA. By Raman spectroscopy, formation of Li_2O_2 is confirmed from the discharged cathode surface, and characteristic peaks of Li_2O, Li_2CO_3 and LiOH are not detected. The results suggest that the major discharged products is Li_2O_2.

By charge, Li_2O_2 became small, but not completely disappeared. From the cross sectional SEM observations, we found that there is still space for the formation of Li_2O_2. It should be noted that there are still discharge products inside the cathode after charge. For the improvements of Li-air battery performance, appropriate design for cathode macro-structure and the identifications of the products formed inside the cathodes will be required. These work are now in progress.

Acknowledgement

The authors thank J. Seki and Y. Akimoto (Toyota Central R&D Labs.) for SEM observations.

References

[1] J. Murray, D. King, Nature 481 (7382) (2012) 433–435.
[2] J.P. Zheng, R.Y. Liang, M. Hendrickson, E.J. Plichta, Journal of the Electrochemical Society 155 (6) (2008) A432–A437.
[3] G. Girishkumar, B. McCloskey, A.C. Luntz, S. Swanson, W. Wilcke, Journal of Physical Chemistry Letters.
[4] P.G. Bruce, S.A. Freunberger, L.J. Hardwick, J.-M. Tarascon, Nature Materials 11 (1) (2012) 19–29.
[5] K.M. Abraham, Z. Jiang, Journal of the Electrochemical Society 143 (1) (1996) 1–5.
[6] J. Read, Journal of the Electrochemical Society 149 (9) (2002) A1190–A1195.
[7] T. Kuboki, T. Okuyama, T. Ohsaki, N. Takami, Journal of Power Sources 146 (2005) 766–769.
[8] F. Mizuno, H. Iba, Meeting Abstract No. 401 of the 219th Electrochemical Society Meeting in Montreal, 1, 14.
[9] B.D. McCloskey, D.S. Bethune, R.M. Shelby, G. Girishkumar, A.C. Luntz, Journal of Physical Chemistry Letters 2 (10) (2011) 1161.
[10] J.S. Hummelshoj, J. Blomqvist, S. Datta, T. Vegge, J. Rossmeisl, K.S. Thygesen, A.C. Luntz, K.W. Jacobsen, J.K. Norskov, Journal of Chemical Physics 132 (2010) 071101.
[11] K. Takechi, S. Higashi, F. Mizuno, H. Nishikoori, H. Iba, T. Shiga, ECS Electrochemistry Letters 1 (2012) A27–A29.
[12] K. Takechi, E. Sudo, T. Inaba, H. Mizuno, F. Nishikoori, T. Shiga, 218th The Electrochemical Society Meeting Abstr (2010), p. 586.
[13] H. Nakamoto, Y. Suzuki, F. Mizuno, H. Nishikoori, K. Takechi, S. Higashi, T. Asaoka, H. Iba, in: Proceeding of 16th International Meeting on Lithium Batteries (IMLB2012), submitted for publication.
[14] H. Sakaebe, H. Matsumoto, Electrochemistry Communications 5 (7) (2003) 594–598.
[15] F. Mizuno, S. Nakanishi, Y. Kotani, S. Yokoishi, H. Iba, Electrochemistry 78 (5) (2010) 403–405.